forests

MDPI

Article

Remote Sensing Assessment and Modeling of the Spatial Dynamics of Tree Stand Disturbance after the Impact of Siberian Silk Moth (*Dendrolimus sibiricus*)

Evgenii I. Ponomarev [1,2,3,*], Evgeny G. Shvetsov [2], Nikita D. Yakimov [2,3], Pavel D. Tretyakov [1,3], Andrey A. Goroshko [1], Svetlana M. Sultson [1,3] and Pavel V. Mikhaylov [1]

1 Scientific Laboratory of Forest Health, Reshetnev Siberian State University of Science and Technology, 31, Krasnoyarskii Rabochii Prospekt, 660037 Krasnoyarsk, Russia
2 Federal Research Center "Krasnoyarsk Science Center, Siberian Branch, Russian Academy of Sciences", 50/45, Akademgorodok, 660036 Krasnoyarsk, Russia
3 Department of Ecology and Environment, Siberian Federal University, 660041 Krasnoyarsk, Russia
* Correspondence: evg@ksc.krasn.ru; Tel.: +7-391-249-4092

Abstract: In this study, we have analyzed tree stand disturbance by hthe Siberian Silk Moth (*Dendrolimus sibiricus* Tschetverikov *(Lepidoptera: Lasiocampidae)*) in Central Siberia (Krasnoyarsk region, Russia) in 2015–2020. We considered two plots that experienced silk moth outbreaks in 2015–2018 and 2018–2020 and used satellite data (Terra/MODIS, Landsat/ETM/OLI), field forest inventory data, a meteorological data set, and a vegetation cover vector layer. Silk moth-disturbed areas were classified using NDVI, which was calculated for each 15-day period during the growing season (April–September). We obtained formalized descriptions of the temporal dynamics of the disturbed area. Next, we classified the degree of disturbance of the forest stand after the impact of the silk moth by the threshold method according to the ranges of NDVI anomalies. Based on the generalized data from the forest inventory, we performed a correlation analysis of the relationship between the main characteristics of forests and the classes of disturbance. Finally, using a series of regression equations, we described a procedure for predicting the degree of impact on the stand during the time of silk moth outbreaks in the dark-needle coniferous stands of Central Siberia.

Keywords: Siberian silk moth; *Dendrolimus sibiricus*; Central Siberia; remote sensing; spatial dynamics model; dark-needle coniferous; tree stand disturbance; NDVI anomalies; regression

Citation: Ponomarev, E.I.; Shvetsov, E.G.; Yakimov, N.D.; Tretyakov, P.D.; Goroshko, A.A.; Sultson, S.M.; Mikhaylov, P.V. Remote Sensing Assessment and Modeling of the Spatial Dynamics of Tree Stand Disturbance after the Impact of Siberian Silk Moth (*Dendrolimus sibiricus*). *Forests* **2023**, *14*, 261. https://doi.org/10.3390/f14020261

Academic Editors: Angela Lo Monaco, Rodolfo Picchio and Mark Vanderwel

Received: 23 December 2022
Revised: 27 January 2023
Accepted: 28 January 2023
Published: 30 January 2023

1. Introduction

Outbreaks of the Siberian silk moth (*Dendrolimus sibiricus*) occur regularly in the dark-needled coniferous forests of Central Siberia. Nine large-scale outbreaks have been recorded in forests of the Krasnoyarsk region of Siberia since 1878 [1]. This is one of the significant factors in the loss of forest stands on a large scale. A number of publications are devoted to the study of this issue in Siberia. Outbreaks are closely correlated with climatic factors, such as long-term periods of drought and prolonged exposure to high temperatures [2,3]. Predicted climate change and global warming create an additional threat of more frequent outbreak events in Siberia. Thus, an expansion of the geoclimatic zone of the Siberian silk moth distribution has been revealed in Siberia during the few last years [4]. However, the potential distribution area of the Siberian (and gipsy) silk moth is much wider and affects the habitats of dark-needled conifers throughout the northern hemisphere [5–8].

The silk moth problem is also studied in various aspects. A number of studies discuss the spatio-temporal dynamics of the silk moth distribution [9–13], methods for monitoring the degree of forest stand disturbance [14–17], relation to the geophysical characteristics of the territory [1,18], probabilistic approaches for predicting an outbreak and the rate of its development [19–21], etc. The results of all known publications are based on the analysis of specific silk moth outbreak events. Thus, predictive solutions, which are associated with a large number of influencing and limiting factors, are still far from being implemented.

An analysis of the pest outbreak development for each specific case requires knowledge of the entire complex of parameters that determine the location, growth rate, and dynamics of the affected area. Previously, it was found [19] that populations of forest insects can be well described by parametric models that predict the population size under various environmental conditions. At the same time, any numerical predictions based on parametric theoretical models must be validated on the basis of field data, which makes it possible to determine the list of model inputs, parameters, and constants [7,22–24]. As for the territory of Siberia, the number of field measurements is usually limited and not always sufficient to calibrate the models that describe the dynamics of the process. For the modern period, the available remote monitoring data may be the only information about the outbreak. When studying insect-disturbed areas, it is also important to study the issue of outbreak locations relative to the physiographic, forest, and meteorological conditions (humidity deficit, precipitation regimes, winter and summer temperature regimes, etc.) of the region. Such important information as forest inventory descriptions for Siberia also has limited availability. This also requires consideration of each individual case [1,7,14,18,22–26].

Regarding the issue, the studies of the disturbed area dynamics that usually leave long-term scars on satellite images are of particular interest. It has been shown [9,27] that after the impact of disturbance factors on forest stands, in particular after the Siberian silk moth outbreak, changes in the spectral characteristics of damaged areas occur [15,28,29]. This determines the prospects for using remote sensing data both for analyzing the forest mortality caused by the complex effects of forest fires, pest outbreaks, etc. [30–33] and for monitoring the dynamics of the spatial distribution of pests. Satellite data also make it possible to perform long-term monitoring of the state of damaged forest stands, allowing classification of the disturbance degree [16,30,34]. Such an approach is now commonly used and widespread in geospatial research in various regions [4,7,11,26].

To assess the state of vegetation cover and to evaluate the degree of disturbance, the most suitable radiometric indices are the normalized difference of vegetation index (NDVI) [29] and land surface temperature (LST) [35]. An anomalous decrease of NDVI compared to the optimal background level is an indicator of tree stand defoliation. This criterion is always used when assessing damage or loss of a stand [29,33]. In addition, anomalous values of the temperature field compared to the background ones can be used to monitor the condition of tree stands after a silk moth outbreak. It has been shown [14] that remotely obtained indicators (NDVI, LST) of stands' susceptibility to environmental changes varied significantly 2–3 years before pest population outbreaks and can be taken into account when assessing the risk of outbreaks.

Thus, we focused our current research on two areas: (i) the spatio-temporal dynamics of damaged areas and (ii) the classification of tree stand disturbances. The spatio-temporal model of the silk moth outbreak development allows estimating the growth rate of the total area and the main tactical elements of the disturbed area. The results of such studies are the basis for further analysis of the parameters that determine the predominant directions of outbreak propagation under conditions of local relief, aspect, and forest growing conditions. At the same time, tree stand damage classification using remote sensing is one of the most important data sets to formalize regressions for silk moth spatial distribution.

We investigated the following issues: (i) the rate of pest outbreak development in dark coniferous forests of Siberia; (ii) modeling the rate of disturbed area increase; and (iii) a correlation analysis of data on disturbance of forest stands with forest inventory characteristics.

The obtained solutions make it possible to have a predictive model for the formation and development of the disturbed forest zone, which is necessary at the stage of planning appropriate preventive measures and developing a general strategy for minimizing the consequences under the conditions of repeated outbreaks of Siberian silk moth in the studied territory.

2. Materials and Methods

2.1. Study Area and Silk Moth Outbreaks

The studies were performed for two sites in the Krasnoyarsk Region, Central Siberia, Russia: (1) in the Yenisei District plot (YnP), with a total area of 4.2 million ha (58°30′–60° N, 88°30′–92° E); and (2) in the Irbei District plot (IrP), with a total area of 904 thousand ha (54°45′–55°05′ N, 95°20′–99°10′ E) (Figure 1).

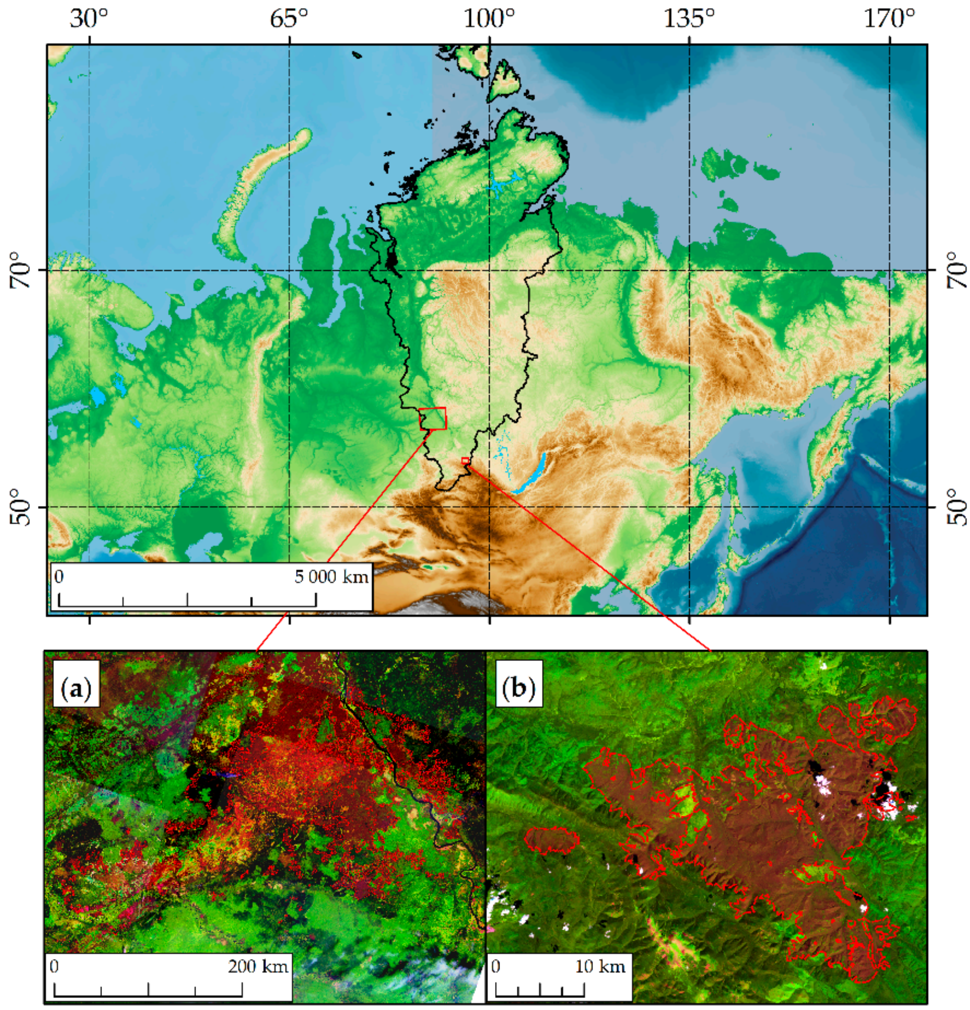

Figure 1. Study area in Krasnoyarsk region (Central Siberia, Russia) and overview of forests disturbed (red outline) by Siberian silk moth from Landsat-8/OLI data for 2020: (**a**) Yenisei District plot (YnP); (**b**) Irbei District plot (IrP).

Dominant tree stands were controlled based on the materials of the "Vega-service" (Database of the Institute of Space Research of the Russian Academy of Sciences, IKI RAS, Moscow, http://pro-vega.ru/maps/, accessed on 15 December 2022) [36].

The territory of the Yenisei Forestry (Yenisei District plot) is located in the east of the West Siberian Plain (Figure 1a). The zonal type of vegetation is the taiga. In the north, the middle taiga subzone is distinguished. The middle and southern parts of the Yenisei region belong to the southern taiga subzone. The main forest stands are fir-spruce-pine (*Pinus sylvestris*, *Abies sibirica*, and *Picea obovata*) forests with large tracts of pure pine forests (∼23% of the total forest area) and Siberian pine (*Pinus sibirica*) forests (up to 17%). Spruce and fir make up 10% of the region's forests. There are also many secondary aspen-birch (*Populus tremula* and *Betula* spp.) forests (more than 40%).

Irbei District plot is located in the southern mountain taiga zone of the East-Sayan mountains (Figure 1b). The territory is dominated by dark-needled conifer (DNC) tree stands (*Pinus sibirica, Abies sibirica,* and *Picea obovata*), which together make up 40% of the forest area of the district. Deciduous (*Populus tremula* and *Betula* spp.) species are dominated by birch stands (about 19% of the territory). Light conifer pine forests (*Pinus sylvestris*) and larch forests (*Larix sibirica*) occupy 16% and 6.5% of the territory of the Irbei Forestry, respectively. Up to 14% of the area in the northwest of the forest is not covered with forest. High-density stands are represented mainly by Siberian pine (*Pinus sibirica*) [1].

In both areas, the damage zone was identified in stands with dominant Siberian pine, spruce, and fir (∼96% of the total area of forest stands). Siberian Silk Moth (*Dendrolimus sibiricus* Tschetverikov, (*Lepidoptera: Lasiocampidae*)) outbreaks were observed between 2016 and 2020 [1,18].

2.2. Initial Data

The initial data on the areas of disturbed forest zones detected by their spectral features were obtained from Landsat data of moderate spatial resolution (15–30 m) with a frequency of 1–3 months and from Terra/Aqua MODIS data of low spatial resolution (250 m) with a frequency of 16 days (standard product MOD13Q1/MYD13Q1) [16]. Thus, in the case of moderate resolution data, the temporal resolution of satellite data for the region of interest was at least once a month. The use of MODIS Vegetation Indices from both the TERRA and AQUA satellites allowed for an 8-day temporal resolution. We used data from the periods 2017–2020 for the Irbei Forestry and 2014–2018 for the territory of the Yenisei Forestry.

A vegetation cover map was obtained from "Vega-service" (Institute of Space Research of the Russian Academy of Sciences, IKI RAS, Moscow) [36]. The resolution of the vegetation map is 230 m. We used the MODIS burned area product (MCD64A1) [37] to detect and exclude fire-disturbed sites from further analysis.

We used CRU TS (Climatic Research Unit Time-Series) climatic datasets of version 4.05 [38] (http://www.cru.uea.ac.uk, accessed on 12 December 2022) to assess the relationship between silkmoth-caused disturbance degree and weather conditions. These datasets are distributed as regular grids with a 0.5° spatial resolution and a temporal resolution of 1 month.

Refined inventory data for Siberian forests is not regularly available. In this work, we updated the data on forest stand composition and taxation characteristics using a vector layer of forest taxation characteristics on the scale of forest network plots (more than 2000 forest network plots in total) of a part of the Irbei Forestry with reference to the Siberian silk moth infestation zone. The initial information is updated at the Forest Protection Center of the Krasnoyarsk Territory (Krasnoyarsk, Russia) (https://krasnoyarsk.rcfh.ru/, accessed on 12 December 2022). The results of the classification of satellite imagery for the Irbei Forestry area were analyzed in conjunction with the forest inventory data for the forest network plots.

2.3. Methods

(1) Data processing and NDVI calculation

All Landsat data were preliminarily radiometrically calibrated for each channel from the metadata file of Landsat data [39]. Converting images to spectral radiance values (https://www.usgs.gov/landsat-missions/using-usgs-landsat-level-1-data-product, accessed on 24 January 2023) allows comparison of mosaics of different satellite images (e.g., Landsat-4, -5, -8) [40], and increases the reliability of the classification results. The NDVI calculation procedure is shown in Figure 2.

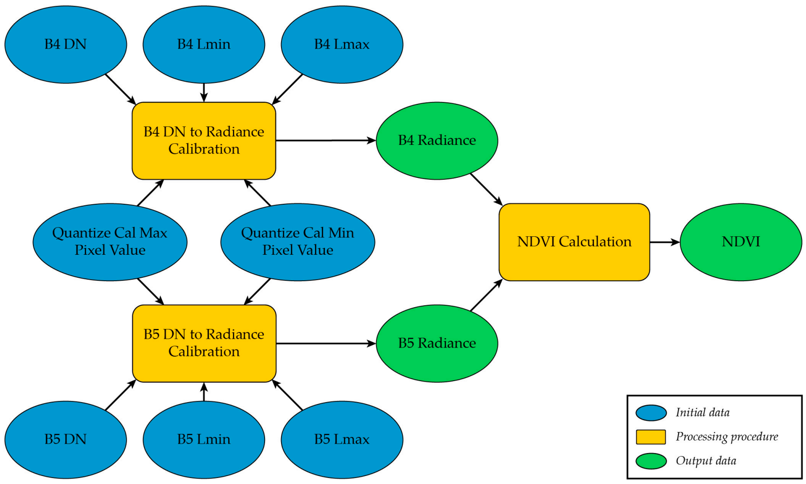

Figure 2. Flowchart for NDVI calculation from Landsat imagery using a GIS technique. Blue elements represent raw data (B4 and B5 are Digital Number data DN from Band #4 and Band #5, respectively; Lmin/Lmax and Quantize Cal Min/Max Pixel value are metadata of Landsat); orange elements represent procedures used; and green elements indicate intermediate and final values.

At the same time, we performed an assessment of the forest disturbance degree using the MODIS vegetation index products MOD13Q1/MYD13Q1. The NDVI index was calculated for the period of the highest photosynthetic activity of vegetation, covering the period from June to September of each year (145–265 days of the year).

The comparison of the NDVI values derived from low-resolution (MODIS) and moderate-resolution (Landsat) satellite imagery was performed on the basis of individual forest network plots. To perform such a comparison, we performed the following procedure: (1) we selected the subsets of MODIS/Landsat pixels located within each forest network plot using GIS tools (Quantum Geographic Information System, version 3.16.3, https://www.qgis.org, accessed on 25 August 2022); (2) we excluded low quality (cloud contaminated) pixels; and (3) we calculated mean NDVI values for the forest network plot.

(2) Classification of disturbance degree

The disturbance degree for each MODIS pixel was estimated based on the comparison of the NDVI value relative to the NDVI value before the outbreak, i.e., the undisturbed state:

$$DD = 100\% \times (NDVI_{pre} - NDVI_{post})/NDVI_{pre},$$

where DD stands for disturbance degree, $NDVI_{pre}$ is the NDVI value before the disturbance, and $NDVI_{post}$ is NDVI value after the disturbance degree.

At the first stage, using data for the zone of disturbances (considering the change in spectral features for the dead forest stands), we classified the forest network plots that were disturbed at least partially. Forest network plots where forest disturbance was not observed using satellite data were classified as background. Further, the disturbed forest network plots and the background ones were compared considering the prevailing forest stands. The disturbance degree was estimated in terms of the relative anomalies of the value of the NDVI for different tree stands. For the YnP plots, information on the scale of forest network plots was not available. The disturbed areas were grouped according to the prevailing stands of dark coniferous species. Data on forest stands were obtained from the vector layer of the Vega Service [36].

(3) Forest inventory data preprocessing in GIS

The analysis of the influence of forest inventory characteristics included such variables as area (S), average stand age (A, years), average stand height (H, meters), average stand diameter (D, sm), stand age class (A_class), stand age group (A_gr), bonitet/quality class

(BC), stock of stands per m^2 (M, m^3/m^2), relative fullness of stands (V = M/M$_{model}$), as well as slope steepness (Sp, degree) (Table 1). All stand characteristics were converted to numerical values. In particular, we assigned numerical values for the categorical variables (dominant tree species, forest type) for which the correlation coefficient was calculated. In the case of species composition, the numerical value was calculated as the proportion of dark coniferous forest stands (Siberian pine, fir, and spruce) within the forest stand.

Table 1. Generalized forest inventory characteristics of the study area (mean value <i> and standard deviation SD).

	S	A, yr	H, m	D, sm	A_Class	A_gr	BC	V	M	Sp, deg
					IrP					
<i>	34.2	120.9	19.28	23.88	5.6	2.8	3.5	0.18	215.2	3.56
SD	42.9	54.13	5.73	9.78	2.11	1.12	0.60	0.39	117.90	7.69
					YnP					
<i>	26.86	139.37	18.26	23.54	6.12	3.11	3.86	0.56	174.26	0.44
SD	30.37	61.38	5.17	8.27	2.3	1.03	0.83	0.13	70.95	2.15

Forest inventory datasets were available only for the disturbed area in the Irbei Forestry plot. The conjugation of the results of satellite imagery classification and forest inventory data was performed only for this area.

(4) Correlation analysis

The assessment of the disturbance degree was analyzed in relation to the physical-geographical, orographic, forest inventory, and geophysical parameters at the scale of sections of the Irbei Forestry of the Krasnoyarsk Territory. The characteristics of the forest network plots used in the analysis included the stand species composition, average stand age, average stand height, average stand diameter, as well as aspect, slope steepness, and mean elevation above sea level. The relationship between the disturbance degree of forest network plots and meteorological variables, such as anomalies in air temperature and precipitation, was also considered. We considered the following variables: (1) temperature and precipitation anomalies for the "current" month (i.e., the month when the largest part of the forest network plot was disturbed); (2) temperature and precipitation anomalies for the "previous" month (i.e., the month preceding the month when the largest part of the forest network plot was disturbed). Air temperature and precipitation anomalies were calculated monthly as a deviation from the long-term average for the 30-year period 1985–2015.

To perform correlation analysis, we have divided the whole sample of forest network plots into training (80% of samples) and test (20%) parts. The training part was used to obtain the regression coefficients, and the test part was used to estimate the performance of the regression equation.

For correlation analysis, this variable was converted to a numerical format. The category values were assigned the following numerical values: 1 is Fir, 2 is Siberian pine, 3 is Spruce, 4 is Birch, and 5 is Aspen.

(5) Multiple regression

The variables with the highest correlation coefficients with the degree of disturbance were included in the multiple regression equation. The coefficients for the model were optimized using the Lagrange multiplier method and non-linear generalized downgrading gradient method (a standard procedure in MS Excel, 2013, 15.0.4569.1504).

3. Results

3.1. Dynamics of the Silkmoth Outbreak Area According to Remote Data

The dynamics of the area disturbed by silk moth in the YnP and IrP plots were calculated using the previously described approaches. The duration of the outbreak in the

YnP was 4 years, while for the IrP it was 3 years. The final disturbed areas were 428.6 and 41.5 thousand ha, respectively (Figure 3).

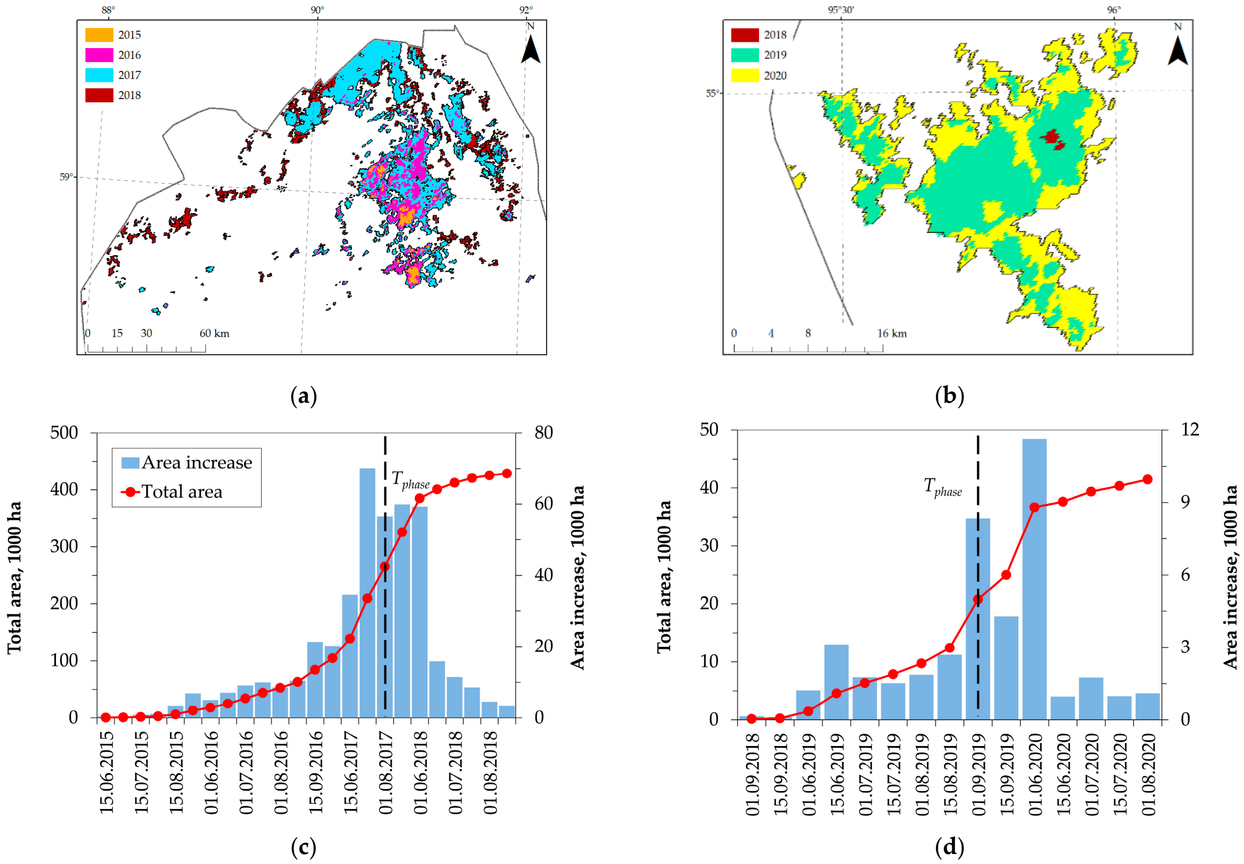

Figure 3. The dynamics of area disturbed by the Siberian silk moth in YnP in 2015–2018 (**a**,**c**) and in IrP in 2018–2020 (**b**,**d**). Evaluated from Terra/MODIS data.

The overall appearance of the area growth histogram and total area increase leads us to conclude that the spatial development of the area disturbed dynamics has a quasi-normal distribution [41]. A similar distribution profile was obtained for another silkworm event in Siberia [11]. Thus, it is theoretically possible to use the normal distribution equation to describe the dynamics of the damaged area. The temporal dynamics of the total disturbed area (Figure 3c,d) can be approximated using the function of normal distribution as follows:

$$f(x) = \frac{1}{\sigma\sqrt{2\pi}} e^{-\frac{(x-\overline{x})^2}{2\sigma^2}}, \quad (1)$$

where $\overline{x}$ is expected value and σ is standard deviation.

However, local perturbations will be present in every silkworm outbreak event. Therefore, we did not test the normality of the distribution, and we proposed to consider different phases using a set of simpler functions (2).

Analyzing the general patterns of the development of the silk moth-disturbed area, two phases can be distinguished that reflect the rate of the geospatial spread of the disturbance:

(a) a phase of increasing growth of disturbed area, which is limited by the time T_{phase} characteristic, which is unique for each case, and is determined by a change in the pattern of growth of the disturbed area;

(b) the phase of the decreasing rate of area growth and further "saturation" (the maximum value of the disturbed area for the given case).

In the case of the IrP, the value of T_{phase} for the time series was 42–46 weeks (until September 2019), the initial area of the disturbed forest was 109.4 ha, and the approximate maximum of the area (the asymptote) was about 35,000 ha. In the case of the YnP, the value of T_{phase} for the time series was 108–110 weeks (until August 2017), and the approximate maximum of the area (the asymptote) was about 430,000 ha (Figure 3).

The type of distribution allows extrapolation of the disturbed area, $S = S(t)$, for each phase as an independent function. The general type of the model can be formulated as follows:

$$S\ (t) = \begin{cases} S^{\mathrm{ph1}} = A\ exp(Bt + C) + D,\ \text{for } t < T_{\mathrm{phase}} \\ S^{\mathrm{ph2}} = E\ ln(Ft + G) + H,\ \text{for } t \geq T_{\mathrm{phase}} \end{cases} \tag{2}$$

and the corresponding set of coefficients (K_i), which determine the amplitude of the initial phase of the disturbed zone's development (A), the rate of area growth (B, F), the state of the disturbed zone at the time of the beginning of logarithmic growth (E), and additive terms (C, D, G, H). Here, the phase of the increasing rate of area growth (exponential increase) is designated S^{ph1}, and the phase of the decreasing rate of area growth and further saturation is S^{ph2}.

The solution (Figure 3a) obtained based on the model approximations (2) agrees well with the experimental data set and has a high level of correlation (r$\sim$0.98) (Table 2).

The coefficients for the model were optimized using the Lagrange multiplier method and the non-linear generalized downgrading gradient method. It is shown that the systems of empirical solutions adequately ($R^2 \sim 0.97$–0.98) fit field data and can be used to simulate silk moth outbreaks under similar conditions in dark-needle coniferous stands in Central Siberia (Figure 4).

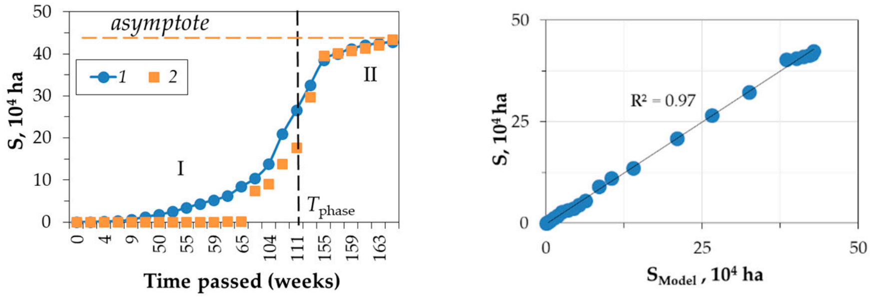

(a) (b)

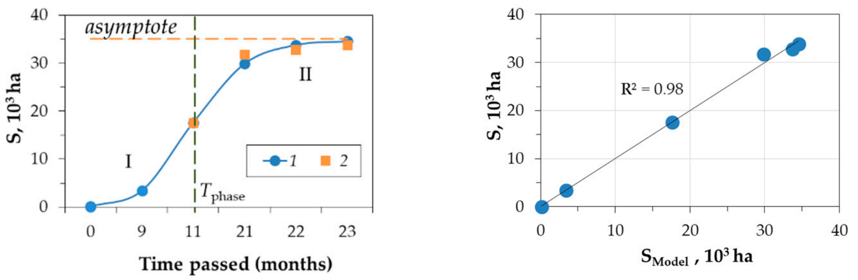

(c) (d)

Figure 4. The dynamics of the area disturbed by silk moth for EnP in 2015–2018 (**a**) and for IrP in 2018–2020 (**b**). Model of the monthly distribution of the area disturbed by silk moth for YnP, which approximates the Terra/MODIS data with 14-day temporal resolution, where I corresponds to exponential growth (phase "I") and II is the approximated final stage. I denoted the experimental data, and II is an approximation of the maximum of the final area. Plots of the correlation field for experimental measurement data (based on satellite data) and model calculation results for YnP (**c**) and IrP (**d**).

Table 2. Coefficients of the equations for the model of disturbed zone growth.

IrP, 2018–2020, T_{phase} = 42–46 Weeks				
Model	**Model Coefficients**			
Phase I: *Aexp(Bx + C) + D*	*A*	*B*	*C*	*D*
	0.91	0.82	0.86	1.00
Phase II: *E ln(Fx + G) + H*	*E*	*F*	*G*	*H*
	22,497.42	0.187	0.07	558.35
EnP, 2015–2018, T_{phase} = 108–110 weeks				
Model	Model Coefficients			
Phase I: *Aexp(Bx + C) + D*	*A*	*B*	*C*	*D*
	0.989	0.100	0.986	1.00
Phase II: *E ln(Fx + G) + H*	*E*	*F*	*G*	*H*
	60.903	0.007	7.704	0.101

3.2. Disturbance Degree Variation

According to Irbei Forestry information, the disturbed area included 85 quarters and 2068 forest network plots. Areas of dominant forest stands are distributed as follows: fir—38.2%, Siberian pine—30.6%, birch—11.6%, aspen—7.2%, spruce—6.1%, pine—5.6%, and larch—0.5%.

In the final stage of the outbreak development, Siberian pine (cedar) occupied the largest area of disturbed dark coniferous stands, which reached up to 50% of the total area (IrP, for the summer season of 2020), and up to 76% of the total area (YnP, for the summer season of 2018). The Siberian pine stands are followed by the fir-dominant forests (up to 33% of the total area in IrP and up to 9% in YnP) and the spruce-dominant forests (5% in IrP and <1% in YnP). Deciduous species such as birch, aspen, and pine made up 13%–15% of the total area for both plots. Larch forests occupied less than 1% of the disturbed area.

The results of the satellite imagery classification were analyzed together with forest inventory data for forest network plots (Figure 5).

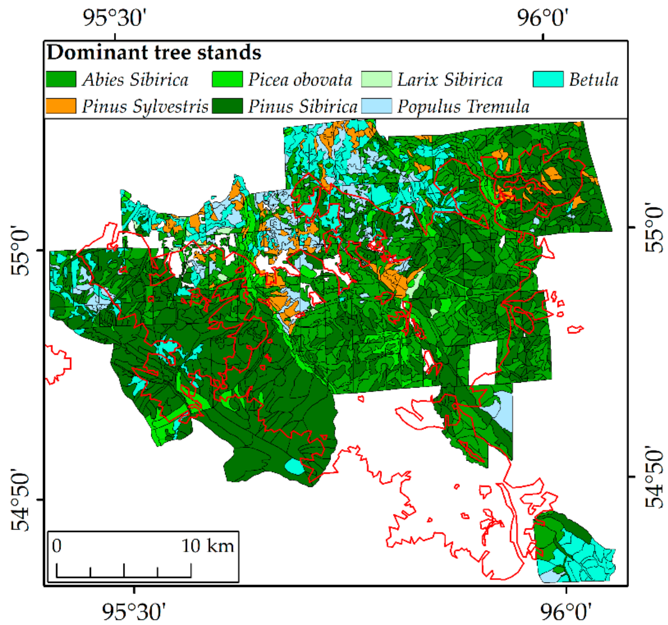

Figure 5. Dominant tree species of the Irbei Forestry. Black lines show forest network plots. The boundaries of the silk moth outbreak are shown in red.

We performed a classification to identify the probabilistic degree of disturbance of dark coniferous stands (classes "fir", "Siberian pine", and "spruce") within the boundaries of forest network plots intersecting with the zone of disturbed forests at the final stage of the outbreak development on 10 August 2020 (Figure 6). Results were obtained from the threshold classification of NDVI data. The thresholds were chosen from the statistics of the values of the relative anomaly of the vegetation index ΔNDVI/NDVIbackground. In addition, we focused on the ranges for different classes of disturbance available from papers on other silk moth outbreak events [4,15].

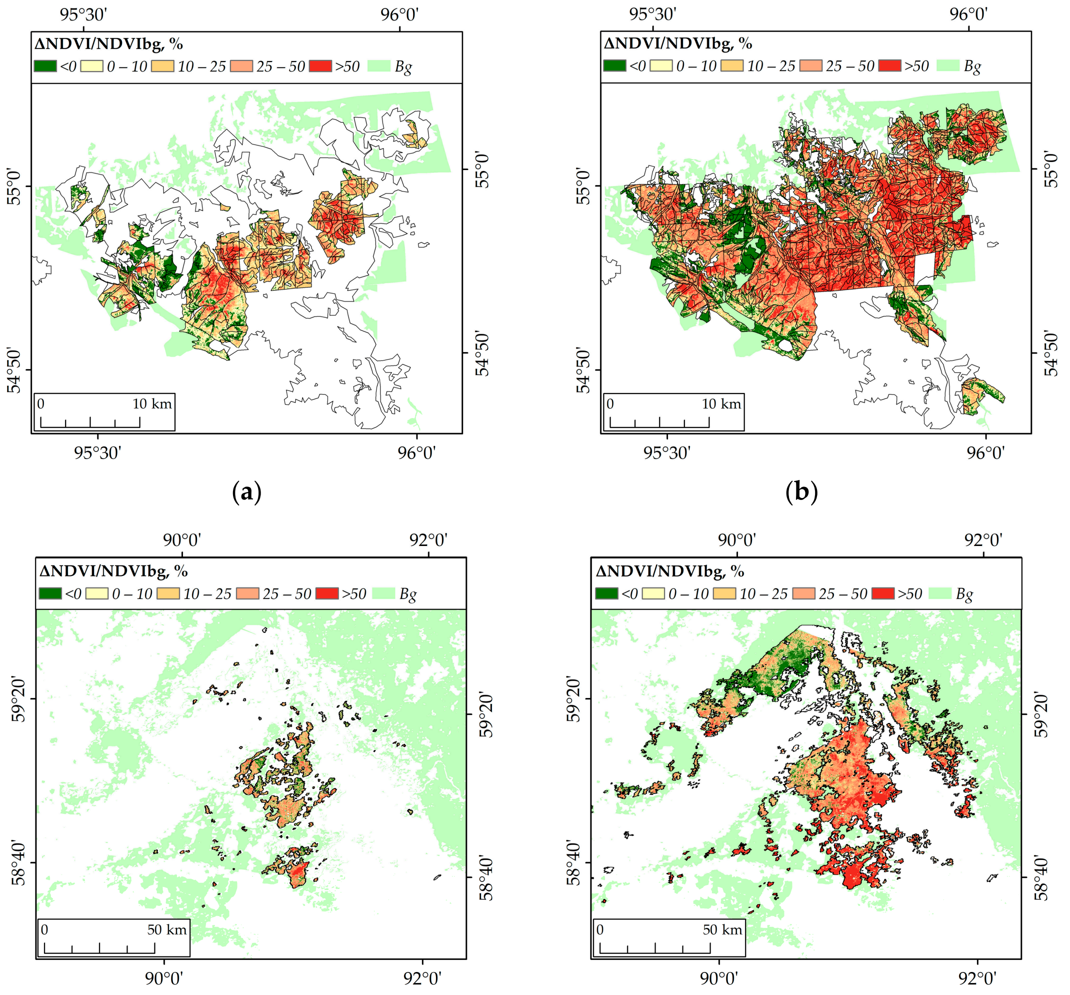

Figure 6. Classification of forest network plots in the Irbei Forestry according to the disturbance degree in terms of NDVI anomaly (%) relative to background for plots with a predominance of "fir", "Siberian pine", and "spruce" classes according to Landsat-8 data for 08/10/2020. Classification of the IrP (**a**,**b**) disturbance zone within forest network plots and YnP (**c**,**d**) by the disturbance degree in terms of NDVI anomaly (%) for plots with a predominance of dark coniferous forests according to Landsat-8 data for 2019 (**a**), 2020 (**b**), 2016 (**c**), and 2018 (**d**).

The classification of forest network plots according to the disturbance degree of forest stands is shown in relation to the level of relative anomaly of the vegetation index $\Delta NDVI/NDVI_{background}$ (Table 3). The selected ranges of values, in our opinion, can be considered as a calibration table of anomalies in the NDVI spectral index, characterizing the disturbance degrees for the DNC forest stands of Siberia.

Table 3. Classification of disturbance degree of the dark coniferous stands considering the anomalies of $\Delta NDVI/NDVI_{background}$ in IrP and YnP.

ΔNDVI/NDVI$_{background}$, %	Disturbance Degree	% of Area			% of Area		
		Fir	Sib. Pine	Spruce	Fir	Sib. Pine	Spruce
		IrP					
		2020			2019		
<0	Minor	12.6	17.8	15.7	2.9	22.8	11.6
0–10	Low	6.3	9.8	10.2	8.5	25.7	21.2
25	Moderate	14.3	14.2	18.3	39.7	27.1	38.3
25–50	High	35.4	36.2	38.1	32.8	17.0	19.7
>50	Extreme	31.3	22.0	17.8	16.1	7.4	9.2
		YnP					
		2018			2016		
<0	Minor	12.7	17.0	–	1.4	21.6	–
0–10	Low	15.4	9.8	–	5.9	17.0	–
25	Moderate	27.6	17.3	–	41.8	24.8	–
25–50	High	28.6	32.2	–	42.4	29.8	–
>50	Extreme	15.6	23.6	–	8.4	6.8	–

3.3. Correlation Analysis

We conducted an analysis of the correlation of forest inventory characteristics and disturbance degree of dark coniferous stands (Siberian pine, fir and spruce) in the Irbei Forestry (IrP) area damaged by the silk moth. Correlations for training forest network plots (80% of samples) are provided in Table 4.

Table 4. Correlation matrix for forest inventory characteristics and disturbance degree (DD).

	Age	Height	Diameter	DTS *	PDNC **	DD
Age	1.00					
Height	0.77	1.00				
Diameter	0.84	0.85	1.00			
DTS *	–0.38	–0.38	–0.14	1.00		
PDNC **	0.60	0.48	0.38	–0.76	1.00	
DD	0.32	0.23	0.19	–0.32	0.36	1.00

* DTS—dominant tree species; ** PDNC—% of dark-needle coniferous stand within forest network plot.

Table 5 shows the correlation matrix relating the silk moth disturbance degree and meteorological variables of the "current" month and the "previous" month (for the training sample).

Table 5. Correlation matrix for weather variables and disturbance degree (DD).

	DT	DP	DTpr	DPpr	DD
DT	1.00				
DP	–0.31	1.00			
DTpr	0.43	–0.14	1.00		
DPpr	0.37	0.32	–0.31	1.00	
DD	0.62	–0.23	0.41	–0.27	1.00

DT—delta temperature (temperature anomaly for the month when the largest part of the forest network plot was disturbed, termed as "current" month); DP—delta precipitation (precipitation anomaly for the "current" month); DTpr—delta temperature for the "previous" month (temperature anomaly for the month preceding the "current" month); DPpr—delta precipitation (precipitation anomaly) for the "previous" month.

Correlation analysis allows us to identify a set of variables that affect the disturbance degree of forest stands within the study area. As such factors, we considered the average stand age (Age), the proportion of dark coniferous species (PDNC), as well as the air temperature for the "current" (DT) and "previous" (DTpr) months (Table 6). The resulting coefficients of the linear regression equation for training forest network plots are presented in Table 7.

Table 6. The list of variables used in regression analysis.

Variable Group	Variable	Variable Type	Description
Dependent	DD	Continuous	The difference in NDVI before and after the disturbance was used as a measure of degree of disturbance
Explanatory	Age	Continuous	Mean age of tree stand within each plot in years
	PDNC	Continuous (from 0 to 100)	Percent of DNC tree species within the plot
	DT	Continuous	Air temperature anomaly for the "current" month, °C
	DTpr	Continuous	Air temperature anomaly for the "previous" month, °C

Table 7. Regression results obtained from Ordinary Least Squares analysis.

Variable	Coefficient	Standard Error	t-Statistic
Intercept	–8.7	2.28	–3.70
Age *	0.13	0.019	6.62
PDNC *	0.20	0.031	6.34
DT *	28.1	1.12	24.91
DTpr *	9.0	1.00	8.96

* An asterisk next to a variable name indicates a statistically significant *p*-value ($p < 0.01$). Multiple $R^2 = 0.51$.

For the second study site, located in the Yenisei Forestry plot (YnP), forest inventory data as a GIS layer were not available. The correlation dependencies will most likely vary from site to site, especially if there are significant differences in orography, local meteorological regime, forest growth conditions, etc. However, this approach when applied in the early stages of outbreak development, can serve as a predictive solution that estimates the probability of disturbed area expansion in relation to the group of input parameters (significant factors) described above.

Using the test sample, we estimated the uncertainty of the obtained regression. The correlation coefficient between the disturbance degree estimated using remote data and the results obtained by the regression equation was 0.49 ($p < 0.05$). Table 8 shows the error matrix of five classes of disturbance degree calculated using the regression equation compared to classes calculated using the NDVI. Obtained regression showed satisfactory overall accuracy (kappa = 0.64).

Table 8. Error matrix for the regression results comparing to NDVI-derived classification. Cell entries are expressed in terms of the number of forest network plots.

		NDVI-Derived Classes					UA
		Minor	**Low**	**Moderate**	**High**	**Extreme**	
Regression-derived classes	Minor	43	8	6	2	3	0.69
	Low	7	28	6	9	4	0.52
	Moderate	6	4	46	12	7	0.61
	High	3	2	7	113	10	0.84
	Extreme	0	1	3	16	76	0.79
PA		0.73	0.65	0.68	0.74	0.76	

PA—producer accuracy; UA—user accuracy.

4. Discussion

4.1. Timeline of Silk Moth Outbreaks

According to the Forest Protection Center of the Krasnoyarsk Territory (Krasnoyarsk, Russia; https://krasnoyarsk.rcfh.ru/, accessed on 12 December 2022), the rise in the number of pests on the territory of the Yenisei Forestry began after insufficient moisture supply in May 2011 and a severe drought in June–July 2012. The hydrothermal regime of the spring-summer period in these years contributed to the early emergence of caterpillars after wintering, their intensive development in June, and the early flight of butterflies. As a result, the pest population entered the prodromal phase of development in 2013.

In 2015, there was a significant moisture deficit in the territory and an excess of the average long-term temperature norm in May. This contributed to the further accelerated development of silkworm caterpillars, the earlier emergence of butterflies, and the emergence of a new generation of pests. The protracted warm autumn of 2015 contributed to an increase in the feeding period of caterpillars. As a result, they left for wintering in the fifth generation. Furthermore, in the summer of 2016, there was a flight of butterfly checks and the population transitioned to the eruptive phase. During this time, the affected area increased from 20,000 hectares to >430,000 hectares [18,25,42].

In the forest stands of the Irbei Forestry, an outbreak of mass reproduction of the Siberian silk worm began in 2015–2016 (the previous one ended in 2004). The exit of the Siberian silk worm population from the depressed state was due to insufficient moisture supply during the growing season of 2015 and June, July, and September of 2016. As a result, in 2017, there was a flight of females with high fecundity and the transition of the pest population to the prodromal phase. The transition of the population to the eruptive phase occurred in the spring of 2019. According to ground and satellite surveys, the first damage to plantations was recorded on an area of >7000 hectares in June 2019. The final stage of disturbance was over 40,000 hectares [1].

4.2. Dynamics of the Silkmoth Outbreak Area

With all the assumptions of the first approximation of the model, the obtained solution for the disturbed area dynamics is in good agreement with the experimental data set and has a high level of correlation, which is shown in the correlation field plots (R^2∼0.97–0.98).

The restrictions imposed on the spatial advancement of the disturbed area are associated with natural boundaries (such as non-forested areas, ridges, valley complexes, rivers, etc.), the heterogeneity of vegetation and forest composition, the time of the outbreak origination, as well as the spatial and temporal peculiarities of the origination of secondary (multiple) locations of pest outbreaks, anisotropy of physical and geographical characteristics, microrelief, and local conditions. Determination of the direction of the predominant advancement of the disturbed area requires a comprehensive analysis of all factors listed above [1,4,7,14,26]. In addition, these indicators can be input conditions that regulate the rate of spread of the disturbed area and individual tactical elements, as well as the degree of damage to forest stands [34].

4.3. Disturbance Degree Variation

The analysis of Landsat-8,-9 imagery in conjunction with standard Terra/MODIS products allows us to define four classes of disturbance degree that can be identified based on the spectral characteristics of forest stands following silk moth impact. The results agree with previously tested approaches [4,14–17] and complement a set of observations of silk moth impact in Siberia.

According to modern publications [4,15], different indices have different sensitivities to the characteristics of stand defoliation. Thus, in [15], the change in the SWVI (Short-Wave Vegetation Index) and NDVI indices in the areas after exposure to the silk moth is compared. In both variants, damaged stands are distinguished by a decrease in indices of 25%–50% relative to the statistical norm: from 0.40–0.42 to 0.25–0.30 for SWVI and from 0.75–0.81 to 0.63–0.68 for NDVI. Based on these dynamics, four categories of forest stand damage can be classified (from slightly damaged to dead) [15].

In a similar way, dead and damaged stands (the only categories of damage) were identified based on the NDII (Normalized Difference Infrared Index) infrared index in the study of Kharuk et al. [4]. NDII values within the range of $0.1 \leq \mathrm{NDII} < 0.3$ were used to detect dead and damaged tree stands. At the same time, the time series of the Enhanced Vegetation Index (EVI) and the differences (Δ) between EVI values within the initial outbreak location and healthy stands were analyzed to evaluate the dead stand's area.

As follows from the publications on the issue, satellite data make it possible to categorize the disturbance of vegetation after the impact of the silk moth. Although these are indirect estimates because ground-based data for the calibration and validation of satellite approaches in Siberia are limited and very often not freely available. That is why the assessment of the state of forest stands is carried out on the basis of an analysis of the statistics of index values and taking into account the previous experience of studies performed for similar conditions.

According to our results, the areas of first-class disturbance ($\Delta\mathrm{NDVI}/\mathrm{NDVI}_{\mathrm{background}} < 0\%$) are characterized by the absence of significant disturbances, where the anomalies of spectral features rapidly decrease due to vegetation regeneration. This group also includes mountainous areas with a low proportion of forest stands and areas obscured by clouds.

The second class of disturbance ($\Delta\mathrm{NDVI}/\mathrm{NDVI}_{\mathrm{background}}$ = 0.01%–10.0%) was assigned to areas with insignificant changes in spectral features.

The third class ($\Delta\mathrm{NDVI}/\mathrm{NDVI}_{\mathrm{background}}$ = 10.01%–25.0%) can be characterized as an average level of disturbance. At the same time, in dark coniferous stands, partial defoliation favors the development of the lower tiers of vegetation. Thus, the level of spectral anomalies can be reduced. Therefore, the disturbance class with $\Delta\mathrm{NDVI}/\mathrm{NDVI}_{\mathrm{background}}$ = 10.01%–25.0% can also be considered critical in predicting the state of dark coniferous stands.

The fourth class ($\Delta\mathrm{NDVI}/\mathrm{NDVI}_{\mathrm{background}}$ = 25.01%–50.0%) is a high level of disturbances, and the fifth class ($\Delta\mathrm{NDVI}/\mathrm{NDVI}_{\mathrm{background}}$ = 50.01%–100.0%) is an extreme level of disturbances. These classes are characterized by the most intense defoliation.

The main forest species affected by the silk moth in central Siberia are fir (*Abies sibirica*) and Siberian pine (*Pinus sibirica*), which are the preferred species, larch (*Larix sibirica*), and spruce (*Picea obovata*) at the peak of an outbreak [43]. Our results are also consistent with this distribution of disturbed areas. Thus, in the southern regions of central Siberia (IrP), most (80%) of the disturbed territory was located in stands of dominant fir and Siberian pine. On the territory of YnP, located to the north of IrP, 84% of the disturbed area was also located in DNC forests.

4.4. Correlations

The degree of forest stand disturbance had the highest correlation coefficients with the following set of variables associated with forest inventory data: (i) mean stand age (0.32) and (ii) proportion of dark coniferous species (0.38). For the other variables considered, the correlation coefficient did not exceed 0.3.

The largest proportion (more than 85%) of disturbed stands was located in the forest network plots where dark coniferous forest stands occupied more than 50% of their area. About 80% of disturbed stands had fir or Siberian pine as dominant forest stands. The mean stand age of disturbed forest network plots (84%) was more than 100 years, while about 47% of disturbed stands were located within plots with a mean stand age between 100 and 150 years. Most of the disturbed plots (89%) were characterized by mean heights ranging from 18 to 27 m and diameters from 18 to 36 cm (83%).

We have not observed any significant correlations between the disturbance degree and relief features. At the same time, Kharuk et al. [4] reported the confinement of tree stands damaged by the Siberian silk moth outbreak to the southern slopes. This was probably caused by the averaging of relief features (slope, aspect) and disturbance degree within the study plots, which led to the loss of information about variations of these variables within each plot. The correlation between the orographic characteristics of sections (mean elevation of forest network plot above sea level, slope aspect, and steepness) and the disturbance degree was insignificant ($r < 0.1$). At the same time, elevation above sea level can be considered a limiting factor preventing silk moth distribution. We did not observe the distribution of silk moth at elevations of more than 850–900 m that is consistent with the results of Kharuk et al. [4], Sultson et al. [1].

Previously, it was found that Siberian silk moth distribution is controlled by air temperature; for instance, the sum of temperatures ($t > +10$ °C) equals 1200 °C, which limits silk moth expansion [42,44]. However, the analysis of climatic variables showed that silk moth expansion is also controlled by monthly temperatures and soil moisture content. It was found [4] that the outbreak onset was promoted by increased dryness, active temperatures, and decreased moisture content within the root zone of soil in the spring-early summer period.

According to our results, the disturbance degree of each forest network plot depends on air temperature anomalies during the month when the disturbance was detected as well as temperature anomalies during the previous month. At the same time, precipitation anomalies showed lower correlation coefficients with the disturbance degree on the monthly time scale. These variables have the largest correlation coefficients with the disturbance degree: (i) 0.63 for the temperature anomaly of the "current" month and (ii) 0.43 for the temperature anomaly of the "previous" month. In general, it can be noted that the period from August to October of 2018–2020 in the study region was characterized by positive air temperature anomalies (with a mean value of ∼1.2 °C). The correlation coefficients for precipitation anomalies were significantly lower.

4.5. Methodology, Extrapolation, and Limitations

The accuracy of the regression model was assessed for a part of the original sample (20% of the total sample size) that was used as test data following methods published by James et al., 2021 [45]. Applying the obtained model to a dataset that was not previously used in model training showed that the model explained about 50% ($R^2 = 0.49$, $p < 0.05$) of the NDVI variance. The overall accuracy of the model, which was evaluated using kappa statistics [46], could be considered satisfactory for the event of the silk moth outbreak in our study (kappa = 0.64).

It should be noted that these results were obtained for a rather small study area. At the same time, it has been previously observed [1,4,14] that the dynamics of pest spread in the forests of Siberia are determined by a set of conditions specific to a particular region. Thus, the direct application of the obtained variables and regression coefficients to other areas probably will not provide correct results. At the same time, since silk moth mainly affects dark coniferous forests [2,4], such a variable as the proportion of dark coniferous stands is likely to remain significant in assessing the distribution of silk moth-disturbed areas in other regions of Siberia. Climate factors are likely to remain significant variables in other regions because they largely determine the distribution of the silk moth [2]. At the same time, the regression coefficients for these variables are likely to change. In addition, it can be assumed that there will be other significant factors that determine the dynamics of the outbreak.

All recent studies [1,4,8,14] of this issue state that the problem of outbreak prediction has a lot of uniqueness in each individual case. The greatest difficulty is predicting the beginning of the outbreak. The model solution of the event requires a large amount of input information [14,17,18,20–25,42]. Moreover, knowledge of probable scenarios of outbreak development, which is available only from field observations under specific conditions, will also be required. However, approaches to assessing the degree of disturbance of forest stands or the total area of a disturbed site are, in our opinion, universal. The use of satellite data has the advantage of providing the ability to monitor the evolution of an outbreak's impact over time [15,16,27,30]. Thus, the approaches described in this article are quite applicable to other silk moth events and/or territories.

5. Conclusions

We obtained formalized descriptions for the temporal dynamics of the area of disturbance for two plots in the Krasnoyarsk region (Siberia, Russia) under the conditions of a Siberian silk moth impact.

Characterization of forest stand disturbance based on the vegetation index $\Delta NDVI/NDVI_{background}$ anomaly is an objective instrumental method for controlling of the silkmoth outbreak development in the event of large-scale damage to dark coniferous stands. Correlation analysis makes it possible to identify a set of factors that characterize not only the spatial distribution of an outbreak under the selected conditions but also the relationship with the probable disturbance degree of forest stands. In our opinion, the general format of such decisions may not change significantly. However, such parameters as the rate of outbreak development and model coefficients, as well as a combination of influencing factors, require consideration in relation to the local features and conditions of each disturbed area of the Siberian dark coniferous taiga. These factors limit the formalization of the general solution and impose conditions on the specification of the characteristics for each case of the Siberian silk moth outbreak.

Author Contributions: Conceptualization, E.I.P.; methodology, E.I.P., N.D.Y. and E.G.S.; software, E.I.P., N.D.Y., E.G.S. and A.A.G.; validation, E.I.P., N.D.Y., S.M.S., P.V.M. and A.A.G.; formal analysis, E.I.P., E.G.S. and A.A.G.; investigation, E.I.P., N.D.Y. and P.D.T.; resources, E.I.P., S.M.S. and P.V.M.; data curation, E.I.P. and S.M.S.; writing—original draft preparation, E.I.P., N.D.Y., S.M.S. and E.G.S.; writing—review and editing, E.I.P. and E.G.S.; visualization, N.D.Y., A.A.G. and P.D.T.; supervision, E.I.P. and S.M.S.; project administration, S.M.S.; funding acquisition, S.M.S. and P.V.M. All authors have read and agreed to the published version of the manuscript.

Funding: This study was partly supported by the Ministry of Education and Science of the Russian Federation (theme: Fundamental principles of forest protection from entomo- and phyto-pests in Siberia; No. FEFE-2020-0014).

Data Availability Statement: Publicly available datasets were analyzed in this study. These data can be found here: http://pro-vega.ru/maps/ (accessed on 21 September 2022) and https://worldview.earthdata.nasa.gov/ (accessed on 22 December 2022).

Acknowledgments: The satellite data-receiving equipment used was provided by the Center for Collective Usage of the Federal Research Center "Krasnoyarsk Science Center, Siberian Branch of Russian Academy of Sciences", Krasnoyarsk, Russia.

Conflicts of Interest: The authors declare no conflict of interest.

References

1. Sultson, S.M.; Goroshko, A.A.; Verkhovets, S.V.; Mikhaylov, P.V.; Ivanov, V.A.; Demidko, D.A.; Kulakov, S.S. Orographic Factors as a Predictor of the Spread of the Siberian Silk Moth Outbreak in the Mountainous Southern Taiga Forests of Siberia. *Land* **2021**, *10*, 115. [CrossRef]
2. Kondakov, Y.P. Mass reproduction of Siberian silk moth. In *Ekologiya Populyatsii Lesnykh Zhivotnykh Sibiri (Population Ecology of Forest Animals in Siberia)*; Nauka: Novosibirsk, Russia, 1974; pp. 206–264. (In Russian)

3. Creeden, E.P.; Hicke, J.A.; Buotte, P.C. Climate, weather, and recent mountain pine beetle outbreaks in the western United States. *For. Ecol. Manag.* **2014**, *312*, 239–251. [CrossRef]
4. Kharuk, V.I.; Im, S.T.; Soldatov, V.V. Siberian silkmoth outbreaks surpassed geoclimatic barrier in Siberian Mountains. *J. Mt. Sci.* **2020**, *17*, 1891–1900. [CrossRef]
5. Kirichenko, N.I.; Baranchikov, Y.N.; Vidal, S. Performance of the potentially invasive Siberian moth Dendrolimus superans sibiricus on coniferous species in Europe. *Agric. For. Entomol.* **2009**, *11*, 247–254. [CrossRef]
6. Foster, J.R.; Townsend, P.A.; Mladenoff, D.J. Spatial dynamics of a gypsy moth defoliation outbreak and dependence on habitat characteristics. *Landsc. Ecol.* **2013**, *28*, 1307–1320. [CrossRef]
7. Möykkynen, T.; Pukkala, T. Modelling of the spread of a potential invasive pest, the Siberian moth (*Dendrolimus sibiricus*) in Europe. *For. Ecosyst.* **2014**, *1*, 10. [CrossRef]
8. Flø, D.; Rafoss, T.; Wendell, M.; Sundheim, L. The Siberian moth (*Dendrolimus sibiricus*), a pest risk assessment for Norway. *For. Ecosyst.* **2020**, *7*, 48. [CrossRef]
9. Im, S.T.; Fedotova, E.V.; Kharuk, V.I. Spectrodiametric satellite imagery in the analysis of the outbreak zone of mass reproduction of the Siberian silk moth. *J. Sib. Fed. Univ. Eng. Technol.* **2008**, *1*, 346–358. (In Russia)
10. Mikhailov, J.Z.; Sumina, N.Y. Siberian moth Dendrolimus superans (Butler, 1877) and control of it in Irkutsk region. *Bajk. Zool. J.* **2012**, *3*, 25–29. (In Russian)
11. Kharuk, V.I.; Demidko, D.A.; Fedotova, E.V.; Dvinskaya, M.L.; Budnik, U.A. Spatial and temporal dynamics of Siberian silk moth large-scale outbreak in dark-needle coniferous tree stands in Altai. *Contemp. Probl. Ecol.* **2016**, *9*, 711–720. [CrossRef]
12. Fomin, S.N.; Barinov, V.V.; Myglan, V.S. Siberian silkmoth in the Republic of Tyva, the history of studies. *Sib. Lesn. Zhurn.* **2019**, *5*, 3–14. (In Russian)
13. Ponomarev, E.I.; Goroshko, A.A.; Shvetsov, E.G.; Yakimov, N.D.; Tretyakov, P.D.; Sultson, S.M.; Mikhaylov, P.V. Spatial Dynamics of Tree Stand Disturbance under Siberian Silk Moth (*Dendrolimus sibiricus*) Impact in Central Siberia in 2016–2020 Based on Remote Sensing Data. *Environ. Sci. Proc.* **2022**, *22*, 4. [CrossRef]
14. Kovalev, A.; Soukhovolsky, V. Analysis of Forest Stand Resistance to Insect Attack According to Remote Sensing Data. *Forests* **2021**, *12*, 1188. [CrossRef]
15. Knyazeva, S.V.; Koroleva, N.V.; Eidlina, S.P.; Sochilova, E.N. Health of vegetation in the area of mass outbreaks of Siberian moth based on satellite data. *Contemp. Probl. Ecol.* **2019**, *12*, 743–752. [CrossRef]
16. Zhirin, V.M.; Knyazeva, S.V.; Eydlina, S.P. Long-term dynamics of vegetation indices in dark coniferous forest after Siberian moth disturbance. *Contemp. Probl. Ecol.* **2016**, *9*, 834–843. [CrossRef]
17. Kovalev, A.V. Analysis of forest stands resistance to Siberian silkmoth attack, according to remote sensing data. *Sib. Lesn. Zhurn.* **2021**, *5*, 71–78. (In Russian) [CrossRef]
18. Pavlov, I.N.; Litovka, Y.A.; Golubev, D.V.; Astapenko, S.A.; Chromogin, P.V. New outbreak of Dendrolimus sibiricus tschetv. in Siberia (2012–2017): Monitoring, modeling and biological control. *Contemp. Probl. Ecol.* **2018**, *11*, 406–419. [CrossRef]
19. Kovalev, A.V.; Ovchinnikova, T.M. Development of simulation models for dynamics of forest pest numbers. *Contemp. Probl. Ecol.* **2010**, *2*, 27–35.
20. Isaev, A.S.; Palnikova, E.N.; Sukhovolsky, V.G.; Tarasova, O.V. *Population Dynamics of Defoliating Forest Insects: Models and Forecasts*; KMK Scientific Press Ltd.: Moscow, Russia, 2015; 262p. (In Russian)
21. Leontiev, D.F. Distribution and forecasting of the population of the Siberian silkmoth (scientific review). *Int. J. Appl. Fundam. Res.* **2015**, *11*, 705–709. (In Russian)
22. Morris, R.F. The development of predictive equations for the spruce budworm based on keyfactor analysis. *Dyn. Epidemic Spruce Budworm Popul. Mem. Entomol. Soc. Can.* **1963**, *95*, 116–129. [CrossRef]
23. Mawby, W.D.; Hain, P.P.; Doggett, C.A. Endemic and epidemic populations of southern pine beetle: Implications of the two-phase model for forest managers. *For. Sci.* **1989**, *35*, 1075–1087. [CrossRef]
24. Iskhakov, T.R.; Sukhovol'skii, V.G.; Ovchinnikova, T.M.; Tarasova, O.V. A population and energy model of a forest insect outbreak. *Biophysics* **2007**, *52*, 440–444. [CrossRef]
25. Lyamtsev, N.I. Assessment and forecast of Siberian moth mass propagation risks in the Krasnoyarsk krai forests. *Izv. St.-Peterbg. Lesoteh. Akad.* **2019**, *228*, 294–311. (In Russian) [CrossRef]
26. Sultson, S.M.; Goroshko, A.A.; Mikhaylov, P.V.; Demidko, D.A.; Ponomarev, E.; Verkhovets, S.V. Improving the Monitoring System Towards Early Detection and Prediction of the Siberian Moth Outbreaks in Eastern Siberia. *Proceedings* **2021**, *68*, 5. [CrossRef]
27. Fedotova, E.V.; Im, S.T.; Kharuk, V.I. Analysis of the spatial confinement of areas of taiga forests disturbed by the Siberian silk moth according to small-scale remote sensing data. *Interexpo GEO-Sib.* **2007**, *2*, 206–210. (In Russia)
28. Wolfe, R.E.; Roy, D.P.; Vermote, E. MODIS Land Data Storage, Gridding, and Compositing Methodology: Level 2 Grid. *IEEE Trans. Geosci. Remote Sens.* **1998**, *36*, 1324–1338. [CrossRef]
29. Didan, K.; Munoz, A.B.; Solano, R.; Huete, A. MODIS Vegetation Index User's Guide (MOD13 Series) Version 3.00 (Collection 6), June 2015. Vegetation Index and Phenology Lab, The University of Arizona. Available online: https://vip.arizona.edu/documents/MODIS/MODIS_VI_UsersGuide_June_2015_C6.pdf (accessed on 1 December 2022).
30. Kharuk, V.I.; Ranson, K.J.; Im, S.T. Siberian silkmoth outbreak pattern analysis based on Spot Vegetation data. *Int. J. Remote Sens.* **2009**, *30*, 2377–2388. [CrossRef]

31. Bartalev, S.; Egorov, V.; Zharko, V.; Loupian, E.; Plotnikov, D.; Khvostikov, S.; Shabanov, N. *Land Cover Mapping over Russia Using Earth Observation Data*; Russian Academy of Sciences Space Research Institute: Moscow, Russia, 2016; p. 208. (In Russia)
32. Kharuk, V.I.; Antamoshkina, O.A. Impact of Silkmoth Outbreak on Taiga Wildfires. *Contemp. Probl. Ecol.* **2017**, *10*, 556–562. [CrossRef]
33. Bartalev, S.A.; Stytsenko, F.V. An assessment of the forest stands destruction by fires based on the remote sensing data on a seasonal distribution of burnt areas. *Contemp. Probl. Ecol.* **2021**, *2*, 115–122. [CrossRef]
34. Vaganov, E.A.; Shashkin, A.V.; Kharuk, V.I.; Khlebopros, R.G.; Sukhovolsky, V.G.; Gaevsky, N.A.; Degermendzhi, A.G.; Gubanov, V.G. *Ecological Biophysics. Vol. 2. Biophysics of Land and Water Ecosystems*; Gitelzon, I.I., Pechurkin, N.S., Eds.; Logos: Moscow, Russia, 2002; 360p, ISBN 5-94010-073-2. (In Russia)
35. Yakimov, N.D.; Ponomarev, E.I.; Ponomareva, T.V. Satellite monitoring of the state and dynamics of disturbed natural and technogenic landscapes in Siberia. *CEUR Workshop Proc.* **2021**, *3006*, 585–593. [CrossRef]
36. Loupian, E.A.; Bourtsev, M.A.; Proshin, A.A.; Kashnitskiy, A.V.; Balashov, I.V.; Bartalev, S.A.; Konstantinova, A.M.; Kobets, D.A.; Radchenko, M.V.; Tolpin, V.A.; et al. Usage Experience and Capabilities of the VEGA-Science System. *Remote Sens.* **2022**, *14*, 77. [CrossRef]
37. Giglio, L.; Boschetti, L.; Roy, D.P.; Humber, M.L.; Justice, C.O. The Collection 6 MODIS burned area mapping algorithm and product. *Remote Sens. Environ.* **2018**, *217*, 72–85. [CrossRef] [PubMed]
38. Harris, I.; Osborn, T.J.; Jones, P.D.; Lister, D.H. Version 4 of the CRU TS monthly high-resolution gridded multivariate climate dataset. *Sci. Data* **2020**, *7*, 109. [CrossRef] [PubMed]
39. Guha, S.; Govil, H. Land surface temperature and normalized difference vegetation index relationship: A seasonal study on a tropical city. *SN Appl. Sci.* **2020**, *2*, 1661. [CrossRef]
40. Teixeira Pinto, C.; Jing, X.; Leigh, L. Evaluation Analysis of Landsat Level-1 and Level-2 Data Products Using in situ Measurements. *Remote Sens.* **2020**, *12*, 2597. [CrossRef]
41. Hawkins, D. *Biomeasurement: A Student's Guide to Biological Statistics*, 3rd ed.; Oxford University Press: Oxford, UK; New York, NY, USA, 2014; 333p, ISBN 978-0-19-965044-6.
42. Kharuk, V.I.; Im, S.T.; Ranson, K.J.; Yagunov, M.N. Climate-Induced Northerly Expansion of Siberian Silkmoth Range. *Forests* **2017**, *8*, 301. [CrossRef]
43. Kharuk, V.I.; Ranson, K.J.; Kozuhovskaya, A.G.; Kondakov, Y.P.; Pestunov, I.A. NOAA/AVHRR satellite detection of Siberian silkmoth outbreaks in eastern Siberia. *Int. J. Remote Sens.* **2004**, *25*, 5543–5555. [CrossRef]
44. Rozhkov, A.S. *Outbreaks of Siberian Silk Moth and Measures of Their Control*; Nauka: Moscow, Russia, 1965; p. 179. (In Russian)
45. James, G.; Witten, D.; Hastie, T.; Tibshirani, R. Introduction. In *An Introduction to Statistical Learning. Springer Texts in Statistics*; Springer: New York, NY, USA, 2021. [CrossRef]
46. McHugh, M.L. Interrater reliability: The kappa statistic. *Biochem. Med.* **2012**, *22*, 276–282. [CrossRef]